Electronic Supplementary Material (ESI) for Nanoscale.

Supporting information

All-wurtzite ZnO/ZnSe Hetero-nanohelix: Formation, Mechanics and Luminescence

L.W. Sun,[a] Z. Z. Ye[a] and H. P. He*[a]

[a] State Key Laboratory of Silicon Materials, College of Materials Science and Engineering, Zhejiang University, Hangzhou 310027, People's Republic of China.

Electronic mail: hphe@zju.edu.cn. (H. P. He)

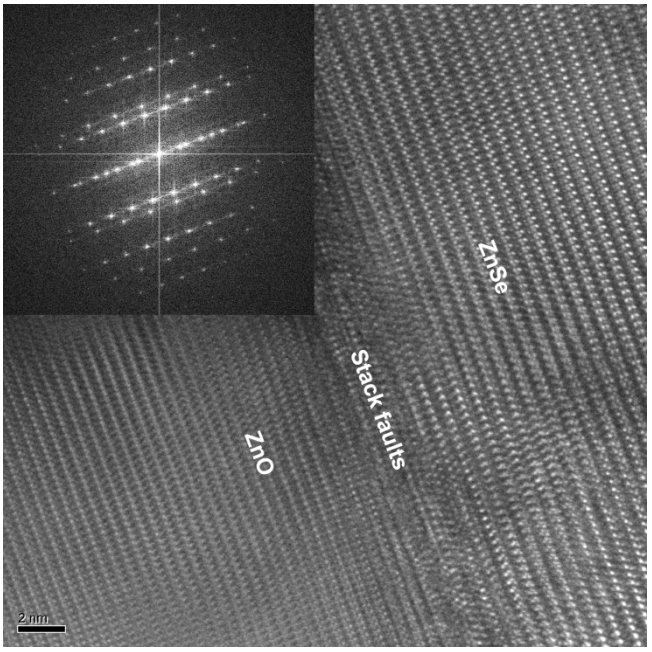

Figure S1 A HRTEM image showing that ZnSe grows on ZnO (0002) planes along [0001] direction; the inset shows a FFT pattern of Figure S6, indicating an epitaxial relationship between ZnO and ZnSe.

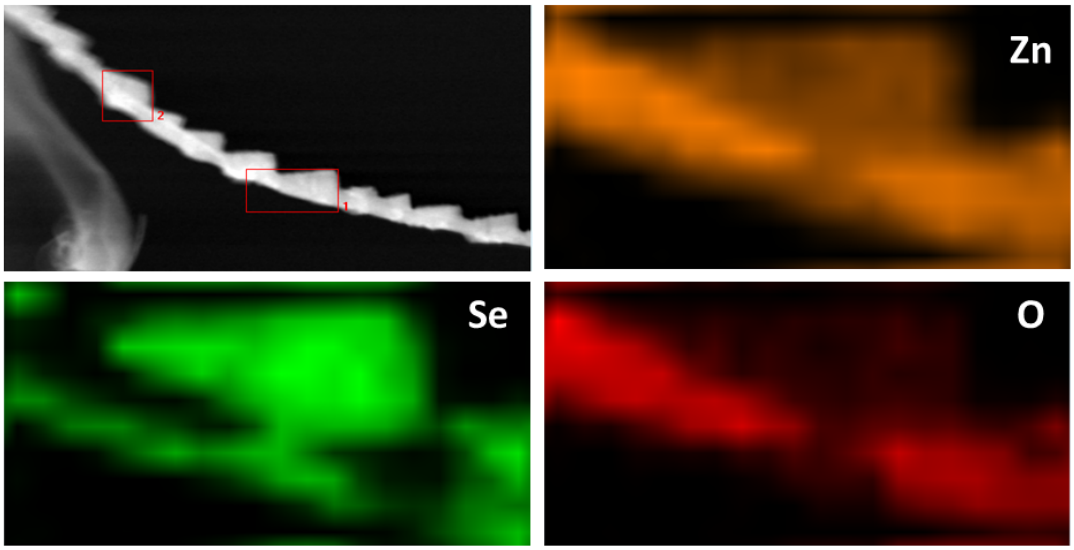

Figure S2 EDS-STEM mapping profiles of ZnO/ZnSe nanohelix. Zinc, Oxygen, and Selenium profiles are obtained from a nanohelix pictured by STEM marked 1 with a red rectangle. Low Oxygen and high Selenium concentration in nanoteeth indicate nanoteeth consist of ZnSe. A contrast decrease in ZnO backbones in Zn profile is tentatively attributed to Selenium dispersion into ZnO nanobelts.

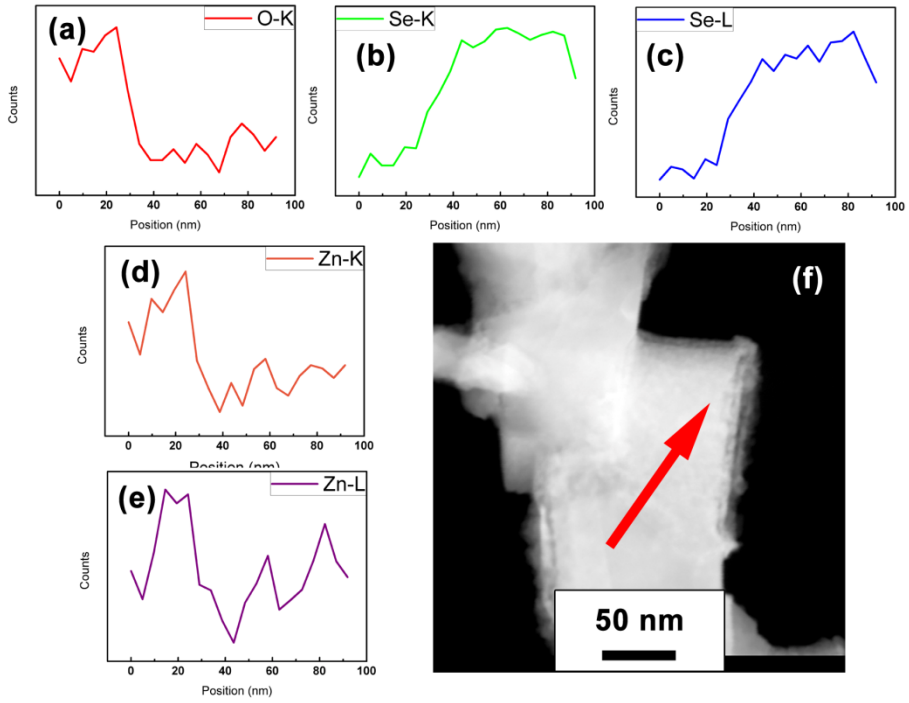

Figure S3 EDS element scanning cross nanohelix. The scanning is performed along the direction a red arrow points in (f). Figure (a) - (e) is element distribution profiles of Oxygen (a), Selenium (b) and (c), Zinc (d) and (e). At 30 nm, oxygen content sharply decrease while selenium content is up gradually, indicating ZnO/ZnSe interface and a transitional layer with a selenium concentration gradient due to selenium dispersion. Zinc profiles in (d) and (e) show a decrease of zinc content due to lower counts above 30 nm, consistent with Se profiles.

Table 1 X-ray diffraction data of ZnO/ZnSe hetero-nanohelix

Wurtzite ZnO (JCPDF Card No. 80-0075)			*Wurtzite ZnSe (JCPDF Card No. 15-0105)*		
$2\theta_{experimental}$	$2\theta_{theoretical}$	(*h l k*)	$2\theta_{experimental}$	$2\theta_{theoretical}$	(*h l k*)
32.02	31.80	(100)	25.73	25.96	(100)
34.66	34.47	(002)	27.20	27.42	(002)
36.43	36.29	(101)	29.07	29.25	(101)
47.80	47.60	(102)	45.45	45.37	(110)
56.82	56.65	(110)	49.46	49.49	(103)
63.10	62.94	(103)	53.68	53.78	(112)
66.62	66.45	(200)	$\Delta\theta = 2\theta_{theoretical} - 2\theta_{experimental}$		
68.10	68.03	(112)	$2\theta_{theoretical}$ (ZnO) is drawn from JCPDF Card No. 80-0075		
69.28	69.16	(201)			
72.91	72.68	(004)	$2\theta_{theoretical}$ (ZnSe) is drawn from JCPDF Card No. 15-0105		
77.13	77.05	(202)			

The analysis of bending mechanics in ZnO nanobelts

(1) The fundamental mechanical parameters of ZnO and ZnSe.

	ZnO	*ZnSe*
a	2.9×10^{-6}/K	7.57×10^{-6}/K
E	140 GPa	67.2 GPa
t	80 nm	75 nm

a: thermal expansion coefficient

E: Young's modulus

t: thickness of each layer

(2) Thermal expansion-induced mechanical bending effect

A mechanical bending model is schematically displayed in Figure S4 and the radius is theoretically estimated as follows.

The bending radius induced by thermal expansion induced mechanical forces is estimated with following expressions:

$$R = \frac{1}{\rho} = \frac{6P\left(t_1 + t_2\right)}{E_1 t_1^3 + E_2 t_2^3} \quad (1)$$

$$P = \frac{\left(a_2 - a_1\right)\Delta T}{\frac{1}{E_1 t_1} + \frac{1}{E_2 t_2} + 3\frac{\left(t_1 + t_2\right)^2}{E_1 t_1^3 + E_2 t_2^3}} \quad (2)$$

ρ: radius of curvature

a: thermal expansion coefficient

E: Young's modulus

t: thickness of each layer

script 1 and 2 correspond to the parameters of ZnSe and ZnO.

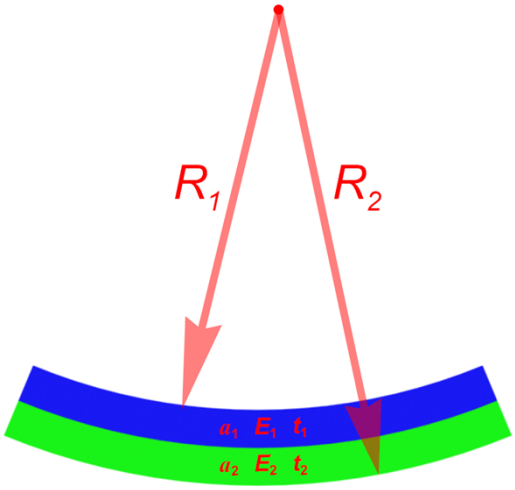

Figure S4. A model showing thermal expansion induced mechanically bending in ZnO and ZnSe where we assume that ZnSe nanorods are deposited on the ZnO nanobelts along [0001] direction and the interface between ZnO and ZnSe is perfect and abrupt.

The radius induced by pure mechanical forces with fundamental mechanical parameters in Table S1 and a temperature change of 800K based on our experiment condition is approximately 181 nm.

(3) The change in electrostatic energy by nanobelts rolling

Figure S5 A model of rolling ZnO nanobelts with polar charges

$$\Delta E_{electro} = \frac{\pi W \sigma^2 R^2}{\varepsilon\varepsilon_0}\left[(1-\beta^2)\ln\left(\frac{1+\beta}{1-\beta}\right)-2\beta\right] \approx -\left(\frac{\pi W \sigma^2}{\varepsilon\varepsilon_0}\right)t^2 \quad (3)$$

W: width of the nanobelts

β=t/2R: t, thickness of nanobelts and *R*, average radius of inner and outer ones

ε: dielectric constant

σ: surface charge density

The energy change originated from polar charges at the surface of ZnO nanobelts is estimated with expression 3 as - 8.02×10^{-13} J.

(4) The change in elastic energy:

$$\Delta E_{elastic} = \left(\frac{\pi W Y}{24R}\right)t^3 \quad (4)$$

W: width of the nanobelts

t: thickness of nanobelts

R: average radius of inner and outer ones

Y: bending modulus

The energy change originated from polar charges at the surface of ZnO nanobelts is estimated with expression 4 as 23.45×10^{-13} J.

(5) The total energy:

$$\Delta E_{total} \approx \Delta E_{electro} + \Delta E_{elastic} \approx -\left(\frac{\pi W \sigma^2}{\varepsilon\varepsilon_0}\right)t^2 + \left(\frac{\pi W Y}{24R}\right)t^3 \quad (5)$$

The total energy is 15.43×10^{-13} J with the calculation by the equation as above.

(6) The maximum thickness-to-radius ratio:

$$\left(\frac{t}{R}\right)^{*} = \left(\frac{24\sigma^2}{\varepsilon\varepsilon_0 Y}\right) = 0.038 \quad (6)$$

$R^* = t^*/0.038 = 4.1$ μm

The most energetically favorable thickness-to-radius ratio:

$$\left(\frac{t}{R}\right)^{0} = \left(\frac{16\sigma^2}{\varepsilon\varepsilon_0 Y}\right) = 0.025 \quad (7)$$

$R^0 = t^0/0.025 = 6.2$ μm